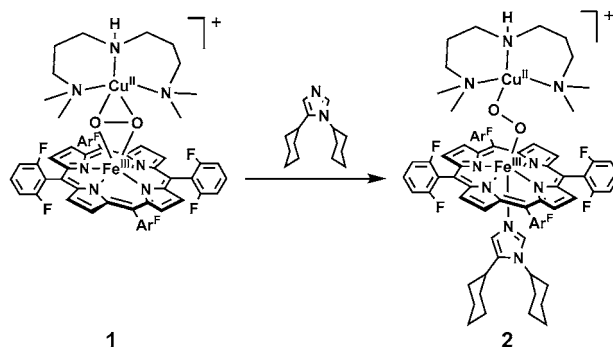


Spectroscopic Elucidation of a New Heme/Copper Dioxygen Structure Type: Implications for O–O Bond Rupture in Cytochrome c Oxidase*

Matthew T. Kieber-Emmons, Munzarin F. Qayyum, Yuqi Li, Zakaria Halime, Keith O. Hodgson, Britt Hedman, Kenneth D. Karlin,* and Edward I. Solomon*

Cytochrome c oxidase (CcO) catalyzes the four-electron reduction of dioxygen to form water in the terminal step of the electron transport chain.^[1] Dioxygen binds to a unique heme–copper bimetallic active site, wherein the copper is ligated about 5 Å above the heme by three His residues.^[2,3] One of these ligating His residues is covalently crosslinked to a nearby Tyr residue. The crosslinked Tyr is thought to participate in catalysis by providing the fourth electron needed to cleave the O–O bond in a net hydrogen abstraction.^[4] This hypothesis stems from the observation of an intermediate state (**P_M**) in CcO that occurs after O–O bond cleavage, which is suggested to contain a tyrosyl radical based on chemical and spectral evidence.^[5–8] The only observable enzymatic dioxygen intermediate before O–O bond rupture has been assigned as a ferric-superoxo species (**A**),^[9,10] leading some to suggest this species is directly responsible for the net hydrogen abstraction from Tyr.^[11,12] We and others favor an alternative mechanistic scenario in which an unobserved peroxo intermediate functions as the active oxidant.^[13–15] A putative peroxo moiety would take advantage of the His–Tyr crosslink and the copper ion as a pathway to access the fourth electron necessary for cleavage of its O–O bond. However, heme–peroxo–copper adducts are generally unreactive towards phenols, thus motivating efforts towards understanding factors required for O–O bond rupture by heme–copper sites. Recently, we reported preliminary evi-

dence that the reaction of a heme–peroxo–copper adduct {[F₈Fe]–O₂–[CuAN]}⁺ (**1**; F₈ = 5,10,15,20-tetrakis(2,6-difluorophenyl)porphyrinate, AN = bis(3-(dimethylamino)propyl)amine) with a coordinating base DCHIm (DCHIm = 1,5-dicyclohexylimidazole) results in formation of a discrete complex (**2**) that has enhanced reactivity towards phenols.^[16] Herein we present the molecular and electronic structure of **2**, which is an example of a heme–peroxo–copper complex in which the electronic state of the heme fragment is low-spin (LS).^[17] Concomitant with the change in spin of the heme fragment from high-spin (HS) to LS upon conversion from **1** to **2**, the Fe–O₂–Cu core undergoes a change from $\mu\text{-}\eta^2\text{:}\eta^2$ (side-on) in **1** to $\mu\text{-}1,2$ (end-on) in **2** (Scheme 1). This novel bridging mode has not been observed previously in heme–



Scheme 1. Reaction of **1** with DCHIm at low temperature to yield a discrete complex **2**.

copper model complexes, but it has been proposed in recent crystallographic studies on resting CcO.^[18–20] However, comparison of the spectral features of resting CcO to those described herein for **2** reveal inconsistencies, suggesting a reevaluation of the bridging mode of the peroxo group in resting CcO and providing insight into the electronic structure requirements for O–O bond cleavage.

Low-temperature reaction of a degassed THF solution of **1** with a molar equivalent of DCHIm generated **2**, as indicated by changes in the optical spectrum (Figure 1). Specifically, a shift in the Soret band from 418 nm ($\epsilon = 133.6 \text{ L mmol}^{-1} \text{ cm}^{-1}$) to 421 nm ($\epsilon = 142.7 \text{ L mmol}^{-1} \text{ cm}^{-1}$) was observed along with a shift and collapse of the split Q band of **1** (λ_{max} [nm] ($\epsilon \text{ [L mmol}^{-1} \text{ cm}^{-1}]$) = 538 (8.4), 561 (6.9)) to 537 nm ($\epsilon = 11.5 \text{ L mmol}^{-1} \text{ cm}^{-1}$) in **2**. While the spectrum of **2** is dominated by the heme spectral features, two low-energy features were observed at 789 nm ($\epsilon = 1.5 \text{ L mmol}^{-1} \text{ cm}^{-1}$) and 951 nm

[*] Dr. M. T. Kieber-Emmons, M. F. Qayyum, Prof. K. O. Hodgson, Prof. E. I. Solomon
Department of Chemistry, Stanford University
Stanford, CA 94305 (USA)
E-mail: edward.solomon@stanford.edu

Y. Li, Dr. Z. Halime, Prof. K. D. Karlin
Department of Chemistry, The Johns Hopkins University
Baltimore, MD 21218 (USA)
E-mail: karlin@jhu.edu

Prof. K. O. Hodgson, Prof. B. Hedman, Prof. E. I. Solomon
Stanford Synchrotron Radiation Lightsource
SLAC National Accelerator Laboratory
Stanford University, Stanford, CA 94309 (USA)

[**] These studies were supported by the NIH (DK031450 to E.I.S., GM60353 to K.D.K., RR001209 to K.O.H.). M.T.K.-E. is supported by an NIH post-doctoral fellowship (GM085914). Computational resources were provided in part by the NSF through Teragrid (CHE080054N). Synchrotron resources were provided by the SSRL, the operation of which is supported by the DOE, Office of Basic Energy Science. The SSRL Structural Molecular Biology program is supported by the NIH (NCRR P41 RR001209) and the DOE Office of Biological and Environmental Research.

Supporting information for this article is available on the WWW under <http://dx.doi.org/10.1002/anie.201104080>.

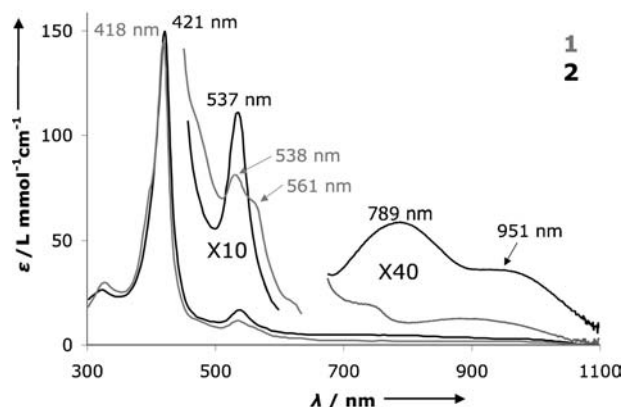


Figure 1. UV/Vis spectra of **1** (—) and **2** (---) at 193 K in THF overlaid with mid-energy region scaled by a factor of 10 and low-energy region scaled by a factor of 40.

($\epsilon = 0.9 \text{ L mmol}^{-1} \text{ cm}^{-1}$). Compound **2** is metastable at 193 K, decaying slowly to $\{[(F_8)Fe]-O-[Cu(AN)]\}^+$ with $\tau_{1/2} = 5 \text{ h}$. **2** is EPR silent, which is consistent with the previously reported ^2H NMR data that indicated a diamagnetic ground state.^[16]

Resonance Raman (rR) studies were performed on **2** over a wide range of excitation energies. Excitation at 413 nm results in a spectrum dominated by heme vibrational features (Supporting Information, Figure S1). Nonetheless, an isotope-sensitive feature was observed at 575 cm^{-1} , which shifted to 552 cm^{-1} in the $^{18}\text{O}_2$ isotopologue. This feature is identical to an isotope-sensitive feature observed in independently prepared $[(F_8)Fe(O_2)(DCHIm)]$, and thus is assigned on this basis as the ν_{Fe-O} of a minor amount ($< 20\%$) of $[(F_8)Fe(O_2)(DCHIm)]$ present in the sample (see the Supporting Information).

In contrast to excitation at higher energies, excitation of **2** at low energy (775 nm) results in observation of five features ($796, 586, 475, 425$, and 394 cm^{-1}), three of which ($796, 586$, and 394 cm^{-1}) shift to lower energy in the $^{18}\text{O}_2$ isotopologue to $754, 561$, and 390 cm^{-1} (Figure 2). These features are not detected upon excitation of **1** or $[(F_8)Fe(O_2)(DCHIm)]$. The 586 cm^{-1} vibration is about five times more intense than the other bands, and it is assigned as an Fe–O stretch on the basis of energy and isotopic shift ($\Delta_{\text{obs(calc)}} = 25 \text{ (26)} \text{ cm}^{-1}$). This energy compares well to the ν_{Fe-O} of a variety of η^1 (or end-on) heme-dioxygen adducts, such as a recent example of a heme-hydroperoxo adduct that has a ν_{Fe-O} absorption at 570 cm^{-1} .^[21] The ν_{Fe-O} band of a η^2 (or side-on) heme-peroxo adduct would be at significantly lower energy, as observed in $[(\text{tmp})Fe(O_2)]^-$ (tmp = 5,10,15,20-tetrakis(2,4,6-trimethylphenyl) porphyrinate) at 470 cm^{-1} .^[21] The 796 cm^{-1} feature is consistent in energy and isotopic shift ($\Delta = 42 \text{ cm}^{-1}$) with assignment as an intra-peroxide stretching mode (ν_{O-O}). The energy of this ν_{O-O} feature in **2** is 40 cm^{-1} higher than that observed for **1**.^[22] The relatively low energy of ν_{O-O} in **1** was defined as resulting from backbonding of the filled copper d orbitals into the strongly antibonding peroxo σ^* orbital in the side-on structure.^[16] Thus, the relatively high energy of the ν_{O-O} mode in **2** is indicative of end-on coordination of the peroxo group to copper. This increase in the ν_{O-O} of the peroxo group upon going from side-on to end-on coordina-

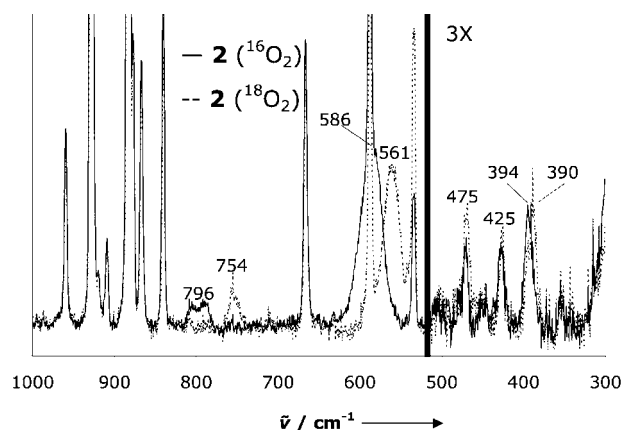


Figure 2. Resonance Raman spectra of **2** prepared with natural abundance O_2 (—) and $^{18}\text{O}_2$ (----) with 775 nm excitation at 77 K in THF. The spectrum presented is the composite of two separate acquisitions on different spots, which is due to the range of the spectral window of the instrument at this excitation energy (separate ranges denoted by thick black bar). The low-energy region has been scaled by a factor of three to aid visualization.

tion to copper is supported by DFT calculations (see below). The isotope shift of the final isotope-sensitive feature at 394 cm^{-1} ($\Delta_{\text{obs}} 4 \text{ cm}^{-1}$) is too small to be a ν_{Cu-O} mode ($\Delta_{\text{calc}} 12 \text{ cm}^{-1}$), and also appears at too low an energy when compared to end-on copper-peroxo dimers, such as $\{[Cu(\text{tmpa})_2(O_2)]^{2+}$ (tmpa = tris(2-methylpyridyl)amine) in which the ν_{Cu-O} mode was observed at 561 cm^{-1} .^[23] The energy of the 394 cm^{-1} band is however consistent with its assignment as a trans-axial δ_{N-Fe-O} bending mode based on an analogous mode observed in $[Fe(\text{BLM})OH]$ (BLM = bleomycin) at 402 cm^{-1} .^[24] Taken together, the rR data indicate that the axial coordination of the imidazole base to **1** causes the peroxo bridge in **2** to adopt a μ -1,2 conformation. Furthermore, the strong enhancement of the ν_{Fe-O} and the lack of a detectable ν_{Cu-O} feature indicate the assignment of the optical band at 789 nm as a peroxo \rightarrow Fe charge-transfer transition.

To verify the coordination mode of the peroxo ligand in **2** and to obtain metrical parameters, Fe and Cu K-edge X-ray absorption spectroscopy (XAS) was performed (Figure 3; Supporting Information, Figures S2, S3, and Tables S1–S5). The XAS data confirm six-coordinate Fe^{III} and four-coordinate Cu^{II} ions, which support a μ -1,2 peroxo bridge spanning the copper and heme derived from the rR data for **2**. Specifically, the first shell of the Fe EXAFS was fitted using one Fe–O/N contribution at $(1.81 \pm 0.02) \text{ \AA}$ and five Fe–N/O contributions at $(2.02 \pm 0.02) \text{ \AA}$. An Fe...Cu contribution was fitted at 3.99 \AA , with its corresponding multiple-scattering (MS) Fe–O–Cu vector refined to 4.08 \AA . However, this Fe...Cu vector was not required in the fit owing to overlap with porphyrin contributions. The Fe K-edge XAS of the independently prepared contaminant $[(F_8)Fe(O_2)(DCHIm)]$ was also separately measured to assess its contribution to the XAS of **2**; subtraction of less than 20% of the contaminant from the spectrum of **2** yielded no significant changes (see the Supporting Information). The first shell of the Cu EXAFS

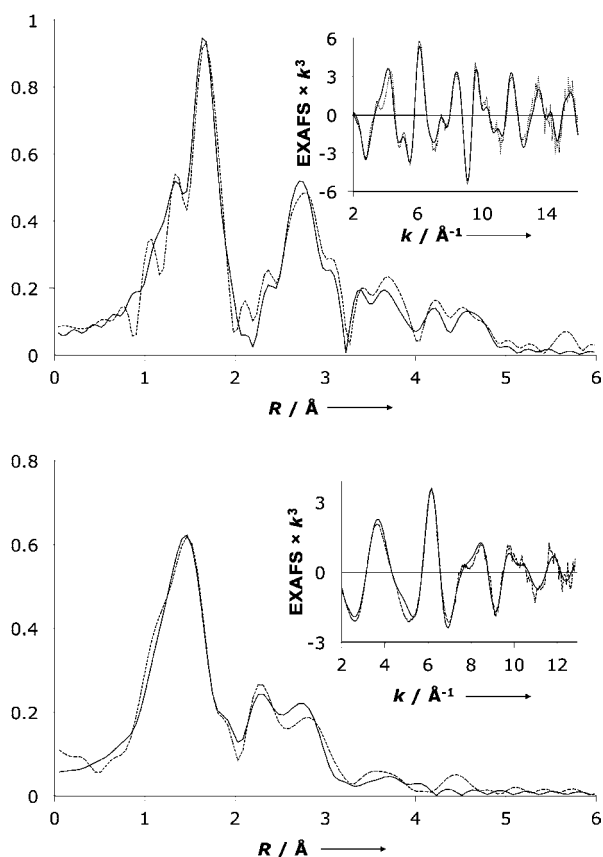


Figure 3. EXAFS (inset) and non-phase-shift-corrected Fourier transform (----) with fit (—) of **2** in THF at 10 K. Top: Fe K-edge (data to $k = 16 \text{ \AA}^{-1}$). Bottom: Cu K-edge (data to $k = 12.8 \text{ \AA}^{-1}$). Phase shifts in the first shells are about 0.4 \text{\AA}.

was fit with four Cu–N/O contributions at $(1.98 \pm 0.02) \text{ \AA}$. Fits wherein the first shell was split to accommodate two scattering paths were not justified based on the resolution of the data (0.14 \AA), but a split shell is consistent with the high σ^2 value, which reflects a distance distribution. The peak in the $R = 3.3\text{--}4.3 \text{ \AA}$ range was fit with a Cu...Fe single-scattering contribution at 4.01 \AA , with its corresponding MS Cu–O–Fe vector at 4.15 \AA ; however, this contribution is also not required by the data.

Density-functional theory (DFT) calculations were performed on **2**. These calculations reproduce its spectroscopically deduced structure where the peroxo ligand bridges the Cu and Fe ions in a $\mu\text{-}1,2$ fashion (Figure 4) and predict that the environment of the iron center is six-coordinate pseudo-octahedral and the copper center is four-coordinate D_{2d} distorted square-planar ($\tau = 47.4^\circ$, where $\tau = 0^\circ$ for square-planar and $\tau = 90^\circ$ for tetrahedral). The peroxidic nature of the bridge is established computationally by a 1.40 \AA O–O bond length, which is significantly shorter than the 1.46 \AA O–O bond calculated for **1**. This decrease in bond length correlates to the DFT calculated $\nu_{\text{O-O}}$ that increases from 821 cm^{-1} in **1** to 840 cm^{-1} in **2**, reproducing the experimental $\nu_{\text{O-O}}$ trend (Supporting Information, Table S8). The computed Fe–O bond length of 1.82 \AA compares well to the EXAFS derived distance of 1.81 \AA , and the Cu–O bond at

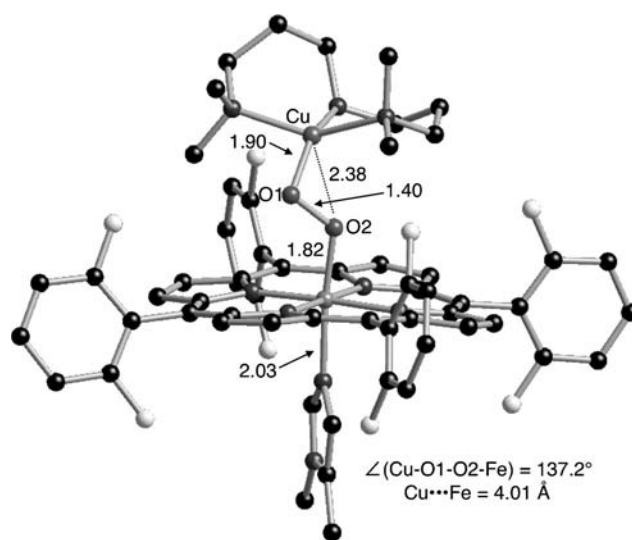


Figure 4. DFT-optimized geometric structure of **2** using the spin-unrestricted BP86 functional on the BS ($S_T = 0$) spin surface.

1.90 \AA compares reasonably to the EXAFS derived Cu–O/N scatterer envelope of 1.98 \AA . The Cu–O bond length of 1.90 \AA is somewhat shorter than the Cu–O bonds in **1** (2.00 and 2.09 \AA), which reflects the change in going from five-coordinate side-on in **1** to four-coordinate end-on in **2**. The Fe–O–O–Cu core dihedral angle is an acute 137.2° , which leads to a relatively short Fe...Cu distance of 4.01 \AA . Compound **2** can be well-described as a broken-symmetry (BS) singlet ($S_T = 0$) that is calculated to be $2.2 \text{ kcal mol}^{-1}$ lower in energy than the triplet, consistent with the diamagnetism observed in the ^1H NMR spectrum. In the singlet state, the low-spin Fe^{III} and the Cu^{II} are antiferromagnetically coupled. The low-spin electronic configuration of the heme is a consequence of the axial ligation of imidazole, and leads to improved donation of the peroxo to iron,^[25] contributing to the strong O–O bond.

Thus, compound **2** is a low-spin heme–peroxo–copper adduct in which the peroxo bridges the metals in a $\mu\text{-}1,2$ fashion. This formulation is based on its spectroscopic features and is supported by DFT calculations. Crystallographic studies on “as-isolated” CcO^[26] have suggested the presence of a bridging peroxo moiety, also in a $\mu\text{-}1,2$ geometry.^[18–20] rR data on the resting enzyme show a feature at 755 cm^{-1} (647.1 nm excitation), which was attributed to an intra-peroxide stretch ($\nu_{\text{O-O}}$) based on its disappearance upon exposure to cyanide.^[27] Isotopically labeled (^{18}O) resting CcO has not been reported, and a ligand–metal ($\nu_{\text{Fe-O}}$) mode is not present in the spectrum ($400\text{--}1200 \text{ cm}^{-1}$). In resting CcO, the heme a_3 is HS ($S = 5/2$) based on the fact that the λ_{max} of the heme Soret band at 424 nm , characteristic of a HS heme^[28] and that SQUID magnetization studies demonstrated the heme $a_3\text{--Cu}_B$ pair are antiferromagnetically coupled to yield an overall $S = 2$ ground state.^[29] Based on the spectral features of the genuine $\mu\text{-}1,2$ peroxo-bridged structure described herein for **2**, the proposed coordination mode of the peroxo moiety in resting CcO is inconsistent with its spectroscopic observables. Specifically, the inconsistencies are: 1) a low intra-peroxide stretch is associated with backbonding from

the copper, where the peroxo σ^* orbital accepts charge from a Cu 3d orbital, which weakens the O–O bond and is only possible for a peroxo bound side-on to a copper as demonstrated in **1** (Scheme 1); 2) end-on coordination of a peroxo to heme in **2** resulted in an intense $\nu_{\text{Fe}=\text{O}}$ that is not observed in resting CcO; and 3) the heme a_3 found in resting CcO is HS despite the strong ligand field expected for a peroxo complex which would result in a LS heme electronic structure, as observed in **2** and in CcO with azide bound.^[30] Taken together, the spectroscopic data of resting CcO require a weak or non-existent interaction of the peroxo with the ferric heme. If the spectroscopic features of resting CcO are correctly interpreted, a more likely coordination mode for the peroxo to Cu is η^2 ,^[31] as in the recent crystallographic structure of a side-on nitrosyl bound to Cu_B in CcO.^[32]

A weak interaction with the heme may also provide insight into the issue of why the peroxo moiety in resting CcO does not reductively cleave to form **P_M**, the intermediate in CcO formed after O–O cleavage. A weak interaction would limit overlap of the Fe d orbitals with the peroxo σ^* orbital and disfavor the electron transfer required for cleavage.^[33] The spin-state change of the heme, which is associated with strong versus weak peroxo interaction with Fe, could also modulate reactivity. Indeed, the spin-state change of HS **1** to LS **2** correlates to the activation of peroxo towards abstraction of the net hydrogen atom from phenol, a prerequisite for reductive O–O bond cleavage. This spin-state change could facilitate this reaction through thermodynamics (an $S=2$ Fe^{IV}=O heme product is disfavored by >20 kcal mol^{−1} compared to an $S=1$ Fe^{IV}=O) and the kinetics associated with the spin-state change. CcO would have additional constraints compared to **2** concerning spin, given the His–Tyr crosslink and proposed magnetic coupling between the Tyr radical and the Cu^{II} ion in **P_M**. Those factors that correlate the HS to LS electronic structure change to reactivity are being further investigated.

Experimental Section

UV/Vis samples were prepared by exposing an equimolar solution of [(F₈)Fe^{II}] (0.36 mM) and [Cu^I(AN)](BAr^F) (0.36 mM) in THF (4 mL) at -80°C to dioxygen to generate **1**. After the removal of the excess dioxygen, 1.0 equiv (100 μL of 14.4 mM, 0.30 mg) of DCHIm was added to yield **2**. rR samples were prepared in 5 mm NMR tubes, sealed with a rubber septum, at 1 mM concentration in an analogous manner. XAS samples were prepared at 5 mM concentration in an analogous manner and loaded into 2 mm Delrin XAS cells with 38 μm Kapton windows. DFT calculations were performed using Gaussian03.^[34] Molecular structures were optimized using the BP86 functional within the spin-unrestricted formalism. The basis sets employed on Fe, Cu, and O₂ were of triple- ζ quality with polarization (6-311g*). A double- ζ quality, split-valence basis was used on all other atoms (6-31g), and was augmented with polarization on the metal bound N atoms (6-31g*). An ultrafine integration grid was employed, as was auto density fitting. Analytical frequency calculations were performed to ensure a stationary point had been reached and no imaginary frequency was found. For additional experimental details, see the Supporting Information.

Received: June 14, 2011

Revised: August 24, 2011

Published online: November 16, 2011

Keywords: copper · cytochromes · dioxygen ligands · heme proteins · Raman spectroscopy

- [1] S. Ferguson-Miller, G. T. Babcock, *Chem. Rev.* **1996**, 96, 2889.
- [2] T. Tsukihara, H. Aoyama, E. Yamashita, T. Tomizaki, H. Yamaguchi, K. Shinzawa-Itoh, R. Nakashima, R. Yaono, S. Yoshikawa, *Science* **1995**, 269, 1069.
- [3] S. Iwata, C. Ostermeier, B. Ludwig, H. Michel, *Nature* **1995**, 376, 660.
- [4] T. K. Das, C. Pecoraro, F. L. Tomson, R. B. Gennis, D. L. Rousseau, *Biochemistry* **1998**, 37, 14471.
- [5] D. A. Proshlyakov, T. Ogura, K. Shinzawa-Itoh, S. Yoshikawa, E. H. Appelman, T. Kitagawa, *J. Biol. Chem.* **1994**, 269, 29385.
- [6] M. Iwaki, J. Breton, P. R. Rich, *Biochim. Biophys. Acta Bioenerg.* **2002**, 1555, 116.
- [7] V. S. Oganessian, G. F. White, S. Field, S. Marritt, R. B. Gennis, L. L. Yap, A. J. Thomson, *J. Biol. Inorg. Chem.* **2010**, 15, 1255.
- [8] D. A. Proshlyakov, M. A. Pressler, C. DeMaso, J. F. Leykam, D. L. DeWitt, G. T. Babcock, *Science* **2000**, 290, 1588.
- [9] C. Varotsis, W. H. Woodruff, G. T. Babcock, *J. Biol. Chem.* **1990**, 265, 11 131.
- [10] S. W. Han, Y. C. Ching, D. L. Rousseau, *Proc. Natl. Acad. Sci. USA* **1990**, 87, 2491.
- [11] J. P. Collman, N. K. Devaraj, R. A. Decreau, Y. Yang, Y. L. Yan, W. Ebina, T. A. Eberspacher, C. E. D. Chidsey, *Science* **2007**, 315, 1565.
- [12] J. P. Collman, R. A. Decreau, C. J. Sunderland, *Chem. Commun.* **2006**, 3894.
- [13] M. R. A. Blomberg, P. E. M. Siegbahn, M. Wikström, *Inorg. Chem.* **2003**, 42, 5231.
- [14] E. E. Chufán, S. C. Puiu, K. D. Karlin, *Acc. Chem. Res.* **2007**, 40, 563.
- [15] D. A. Proshlyakov, M. A. Pressler, G. T. Babcock, *Proc. Natl. Acad. Sci. USA* **1998**, 95, 8020.
- [16] Z. Halime, M. T. Kieber-Emmons, M. F. Qayyum, B. Mondal, T. Gandhi, S. C. Puiu, E. E. Chufán, A. A. Sarjeant, K. O. Hodgson, B. Hedman, E. I. Solomon, K. D. Karlin, *Inorg. Chem.* **2010**, 49, 3629.
- [17] A prior LS example was proposed in J. P. Collman, P. C. Herrmann, B. Boitrel, X. Zhang, T. A. Eberspacher, L. Fu, J. Wang, D. L. Rousseau, E. R. Williams, *J. Am. Chem. Soc.* **1994**, 116, 9783. However, this exhibits too small an isotope perturbation of $\nu_{\text{O}=\text{O}}$ ($\Delta=18$ cm^{−1}). Another LS example was reported in: J. Liu, Y. Naruta, F. Tani, *Angew. Chem.* **2005**, 117, 1870; *Angew. Chem. Int. Ed.* **2005**, 44, 1836, in which the ground state of the heme was inferred based on the porphyrin ν_2 band.
- [18] H. Aoyama, K. Muramoto, K. Shinzawa-Itoh, K. Hirata, E. Yamashita, T. Tsukihara, T. Ogura, S. Yoshikawa, *Proc. Natl. Acad. Sci. USA* **2009**, 106, 2165.
- [19] J. Koepke, E. Olkhova, H. Angerer, H. Müller, G. Peng, H. Michel, *Biochim. Biophys. Acta Bioenerg.* **2009**, 1787, 635.
- [20] T. Tiefenbrunn, W. Liu, Y. Chen, V. Katritch, C. D. Stout, J. A. Fee, V. Cherezov, *PLoS One* **2011**, 6, e22348.
- [21] J.-G. Liu, T. Ohta, S. Yamaguchi, T. Ogura, S. Sakamoto, Y. Maeda, Y. Naruta, *Angew. Chem.* **2009**, 121, 9426; *Angew. Chem. Int. Ed.* **2009**, 48, 9262.
- [22] E. E. Chufán, B. Mondal, T. Gandhi, E. Kim, N. D. Rubie, P. Moenne-Loccoz, K. D. Karlin, *Inorg. Chem.* **2007**, 46, 6382.
- [23] M. J. Baldwin, P. K. Ross, J. E. Pate, Z. Tyeklär, K. D. Karlin, E. I. Solomon, *J. Am. Chem. Soc.* **1991**, 113, 8671.

- [24] L. V. Liu, C. B. Bell, S. D. Wong, S. A. Wilson, Y. Kwak, M. S. Chow, J. Zhao, K. O. Hodgson, B. Hedman, E. I. Solomon, *Proc. Natl. Acad. Sci. USA* **2010**, *107*, 22419.
- [25] In a low-spin heme, the Fe d_{z^2} orbital is completely unoccupied. Thus, donation from the $O_2^{2-} \pi^*$ into this orbital is more effective compared to a high-spin electronic configuration because of the lack of electron–electron repulsion in this bonding interaction.
- [26] The resting “as-isolated” form of the enzyme used for the crystallography is also called the “fast” fully oxidized form. See: A. J. Moody, C. E. Cooper, R. B. Gennis, J. N. Rumbley, P. R. Rich, *Biochemistry* **1995**, *34*, 6838 for an overview of “fast” versus “slow”.
- [27] M. Sakaguchi, K. Shinzawa-Itoh, S. Yoshikawa, T. Ogura, *J. Bioenerg. Biomembr.* **2010**, *42*, 241.
- [28] G. M. Clore, L. E. Andréasson, B. Karlsson, R. Aasa, B. G. Malmström, *Biochem. J.* **1980**, *185*, 139.
- [29] E. P. Day, J. Peterson, M. S. Sendova, J. Schoonover, G. Palmer, *Biochemistry* **1993**, *32*, 7855.
- [30] A. J. Thomson, C. Greenwood, P. M. Gadsby, J. Peterson, D. G. Eglinton, B. C. Hill, P. Nicholls, *J. Inorg. Biochem.* **1985**, *23*, 187.
- [31] The residual density between heme a_3 and Cu_B was also modeled in an earlier study (S. Yoshikawa, K. Shinzawa-Itoh, R. Nakashima, R. Yaono, E. Yamashita, N. Inoue, M. Yao, M. J. Fei, C. P. Libeu, T. Mizushima, H. Yamaguchi, T. Tomizaki, T. Tsukihara, *Science* **1998**, *280*, 1723, footnote 9 therein) as a hydroperoxide bridge with the proton on the iron-bound oxygen atom, thus substantially weakening the peroxo–iron interaction. However, it should be noted that typical Cu–OOH intraperoxo stretching frequencies are more than 820 cm^{-1} .
- [32] K. Ohta, K. Muramoto, K. Shinzawa-Itoh, E. Yamashita, S. Yoshikawa, T. Tsukihara, *Acta Crystallogr. Sect. F* **2010**, *66*, 251.
- [33] An alternative proposal has been presented in V. R. I. Kaila, E. Oksanen, A. Goldman, D. A. Bloch, M. I. Verkhovsky, D. Sundholm, M. Wikström, *Biochim. Biophys. Acta Bioenerg.* **2011**, *1807*, 769, in which the putative peroxo moiety in resting CcO is suggested as a superoxo moiety. However, such a species is inconsistent with the Raman spectral feature and would be LS.
- [34] M. J. Frisch, et al., Gaussian, Inc. Wallingford, CT, **2004**. (For the full reference, see the Supporting Information).